Journal of Applied Sciences

ISSN 1812-5654

science alert

ANSInet
an open access publisher
http://ansinet.com

Journal of Applied Sciences 8 (15): 2758-2763, 2008
ISSN 1812-5654

Comprehensive Study of 2-D and 3-D Finite Element Analysis of a Switched Reluctance Motor

Hossein Torkaman and Ebrahim Afjei
Department of Electrical Engineering, Shahid Beheshti University, Tehran, Iran

Abstract: This study describes the performance characteristics and comparison results of a six by four switched reluctance motor analysis utilizing three-dimensional/two-dimensional finite element method. In the three-dimensional finite element analysis, the end effects and axial fringing fields for simulating reliable model of switched reluctance motor have been considered. The results of the three-dimensional finite element analysis of 6/4 switched reluctance motor such as flux-linkages, terminal inductance per phase, mutual inductance and static torque for various motor conditions are obtained and presented. Finally, these results were compared with the same motor profile using two-dimensional finite element method.

Key words: Switched reluctance motor, SRM, numerical analysis of SRM, 3-D finite element method (3-D FEM)

INTRODUCTION

Exclusive features of the Switched Reluctance Motor (SRM) such as lack of any coil or permanent magnet on the rotor, simple structure and high reliability, makes it a suitable candidate for operation in harsh or sensitive conditions. The different aspects of SRM drives have been extensively investigated and carried out in the past decades by several research organizations (Miller, 1993). Designing SR motor especially for high performance motion control systems, requires accurate knowledge of the magnetic fields that relate motor geometry. Magnetic field simulation directly yields predictions of flux linkages, field energy and torque.

Determination of the magnetic characteristics is a key point to the optimization design and/or control strategy evaluation in a switched reluctance machine. They can be obtained numerically or experimentally. The numerical determination can be based on Finite Element Method (FEM) analysis, conveniently used to obtain the machine magnetic vector potential values in the presence of complex magnetic circuit geometry and nonlinear properties of the magnetic materials (Parreira *et al*., 2005).

In Hannoun *et al*. (2007) is presented an analytical model of the inductance and of the torque, based on the results of a two-dimensional finite element method (2-D FEM) applied to an 8/6 prototype machine. The model takes into account the non linear characteristics due to the magnetic saturation.

The effect of eccentricity fault on the torque profile of an SRM with 2-D FEM has been investigated in Geldhof *et al*. (2007). Dorrell *et al*. (2005) have investigated the effect of eccentricity on torque profile with respect to the switching angle using 2-D FEM. Other researches such as Husain *et al*. (2000), Ozoglu *et al*. (2005), Sheth *et al*. (2006) and Kamper *et al*. (2007) have analyzed SRM based on two-dimensional finite element method.

It is difficult to take into account the magnetic material laws by using a pure two-dimensional finite element method simulation, owing to the high computational cost (CPU time and memory) (Sixdenier *et al*., 2006). This study proposes a comprehensive three-dimensional finite element method (3-D FEM) simulation on 6/4 Switched reluctance motor and then compares its results with a two-dimensional finite element method. The field analysis has been performed using a Magnet CAD package (2007) which is based on the variational energy minimization technique to solve the magnetic vector potential.

FINITE ELEMENT ANALYSIS

A three dimensional finite element analysis is being used to determine the magnetic field distribution in and around the motor. In order to present the operation of the motor and to determine the static torque at different positions of the rotor, the field solutions are obtained. The field analysis has been performed using a Magnet CAD package (2007) which is based on the variational energy minimization technique to determine the magnetic vector potential. The partial differential equation for the magnetic vector potential is (Sadiku, 2000):

$$-\frac{\partial}{\partial x}(\gamma\frac{\partial A}{\partial x})-\frac{\partial}{\partial y}(\gamma\frac{\partial A}{\partial y})-\frac{\partial}{\partial z}(\gamma\frac{\partial A}{\partial z})=J \quad (1)$$

Corresponding Author: Hossein Torkaman, Department of Electrical Engineering, Shahid Beheshti University, Tehran, Iran
Tel: +9821 29902266 Fax: +9821 22431804

where, A is magnetic vector potential and is defined as:

$$B = \nabla \times A \quad (2)$$

B is the magnetic flux density. Considering appropriate boundary conditions, Eq. 1 yields the magnetic vector potential.

In the variational method (Ritz), the solution of Eq. 1 is obtained by minimizing the following functional:

$$F(A) = \frac{1}{2}\iiint_{\Omega}[\gamma(\frac{\partial A}{\partial x})^2 + \gamma(\frac{\partial A}{\partial y})^2 + \gamma(\frac{\partial A}{\partial z})^2]d\Omega - \iiint_{\Omega} JAd\Omega \quad (3)$$

In the three dimensional finite element analysis, a tetrahedral or hexahedral (rectangular prism) element, with dense meshes at places where the field variations are being changed rapidly has been used.

For the present study, it has been assumed that each phase of the motor is excited with four-node tetrahedral blocks of current. Also, in this analysis, the usual assumptions such as the magnetic field outside of an air box in which the motor is placed considered to be zero.

The unaligned position is defined when the rotor pole is located across from the stator slot in such a way that the reluctance of the motor magnetic structure is at its maximum. This position is considered to be at zero degree in the motor performance plot. The aligned position is defined when the rotor pole is fully opposite to the stator pole, in which the reluctance of the motor magnetic structure is at its minimum. This position is assumed to be 44 degrees for the rotor position in the motor performance plots.

In this study, the rotor moves from unaligned to fully aligned position hence, all motor parameters for these points in between can be computed. In order to represent the motor operation and determine the static torque at different rotor positions, the field solutions are obtained at 0, 4, 8, 12, 16, 20, 24, 28, 32, 36, 40 and 44 degrees from the unaligned position. The plots of magnetic flux throughout the motor and parameters have been computed, compared and elaborated upon.

Motor specifications and simulation: The motor specifications and configuration used in this study are shown in Table 1 and Fig. 1, respectively.

The stator and rotor cores are made up of M-27 non-oriented silicon steel laminations with the following static B-H curve shown in Fig. 2.

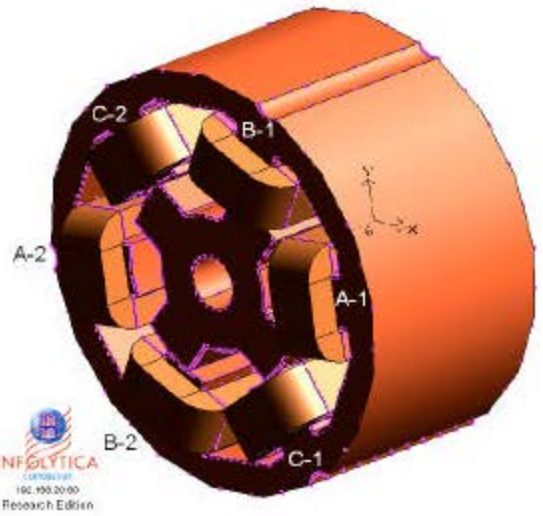

Fig. 1: 6/4 SR motor configuration

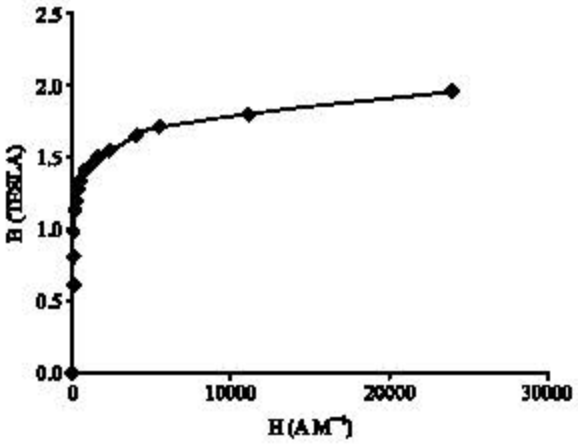

Fig. 2: Magnetization curve for M-27 non-oriented silicon steel sheet

Table 1: 6/4 SR Motor Dimensions

Parameter	Value
Stator core outer diameter	72.0
Rotor core outer diameter	40.5
Length of air gap	0.25
Shaft diameter	10.0
Rotor pole arc	32°
Stator pole arc	28°
No. of turns	120

In this study, each phase winding consists of 120 turns with a current magnitude of 2.5 A. Due to precise comparison between 2-D and 3-D FE analyses, the mesh densities are considered to be exactly the same for both cases. The FE model with mesh densities used in the simulation is as shown in Fig. 3.

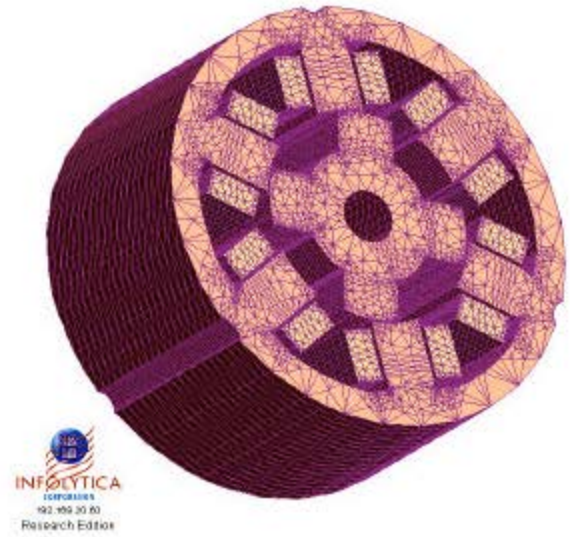

Fig. 3: Finite element mesh for the SRM

NUMERICAL RESULTS

To investigate the magnetic characteristics on the 6/4 switched reluctance behavior, the motor is simulated utilizing 3-D and 2-D finite element analysis.

Flux density shadow and arrows of the motor which is utilizing 3-D FE analysis are shown in Fig. 4.

Flux density shadow and arrows of the motor that is utilizing 2-D FE analysis are shown in Fig. 5.

As expected, the variations in flux density due to the eccentricity with 3-D FEM are larger than those of the 2-D FEM (Fig. 4, 5), which is due to fringing effect for the field that has been disregarded in 2-D FEM. There is 38% increase in the variation in its highest form.

The variation percentage is defined as follows:

$$\text{Variation} = \frac{X_{3D} - X_{2D}}{X_{2D}} \times 100\ (\%) \qquad (4)$$

In the above equation, X_{2D}, X_{3D} are any defined parameter values of 2-D FEM as well as 3-D FEM, respectively.

Flux-linkage/rotor position characteristic is the most important profile of the SRM. Figure 6 shows the flux-linkage of coil one in phase A, utilizing 3-D/2-D FEM vs. variation of the rotor positions.

In addition, Fig. 6 shows that with the overlapping increase between rotor and stator, flux-linkage of coil one of the excited phase will increase.

As shown above, the flux linkage peaks at about 44 degrees, correspond to the rotor pole located completely aligned with the related stator pole.

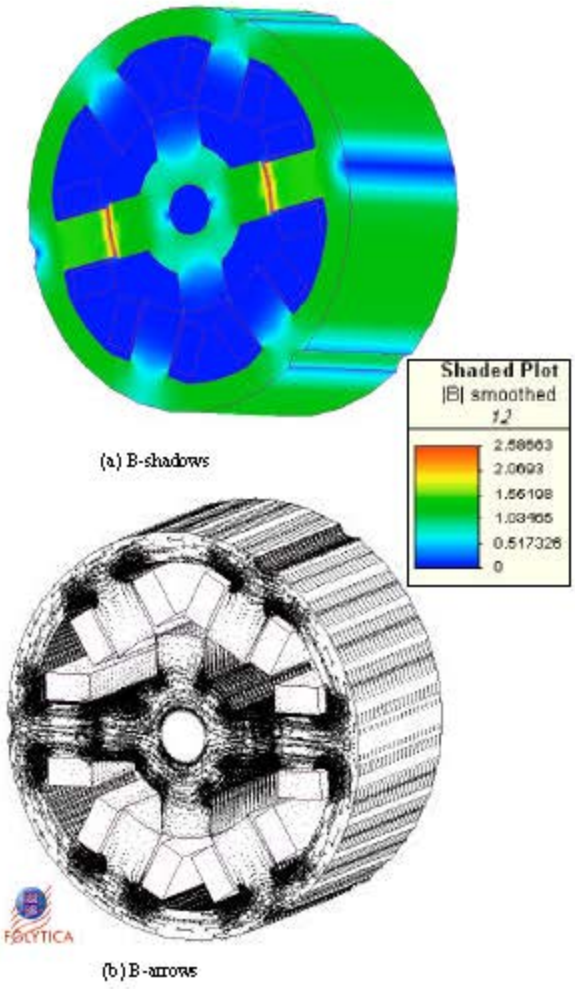

Fig. 4: Flux density (a) shadows and (b) arrows for 6/4 SRM utilizing 3-D FEM

The result of the flux linkages in different rotor positions just like the results obtained from the 3-D analysis, but with a maximum of 19% higher values due to the assumption made in 2-D analysis. The 3-D/2-D FEM comparison results of the flux-linkage variations for coil one in phase A are shown in Fig. 7. The variation percentage for aligned and unaligned positions is from 0 to 19%.

The inductance has been defined as the ratio of each phase flux-linkage to the exciting current (λ/I). Since the inductance is directly proportional to the flux linkage, the resulting inductance values utilizing 3-D FEM for phase A have 19 and 3.6% variations in unaligned and aligned positions, compared with a motor that analyzed utilizing 2-D FEM. This procedure results the same outcomes for other coils in different phases.

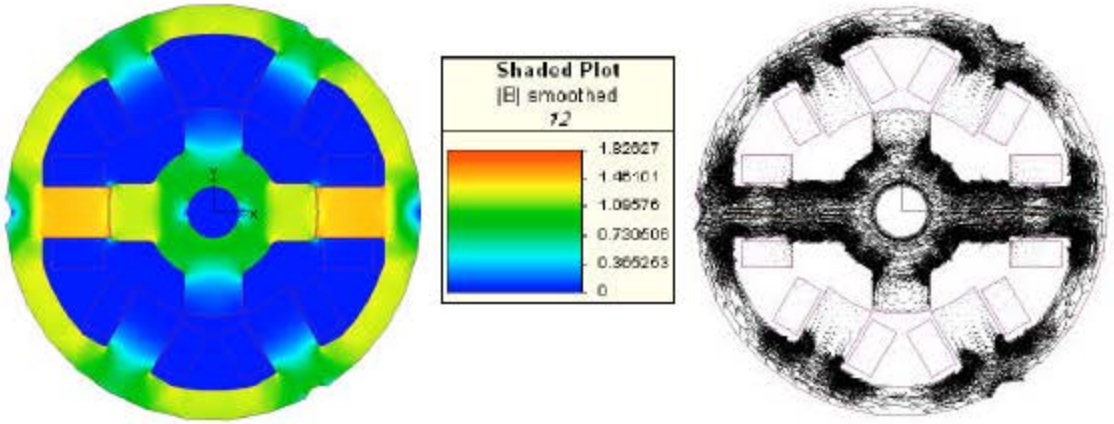

Fig. 5: Flux density (a) shadows and (b) arrows for 6/4 SRM utilizing 2-D FEM

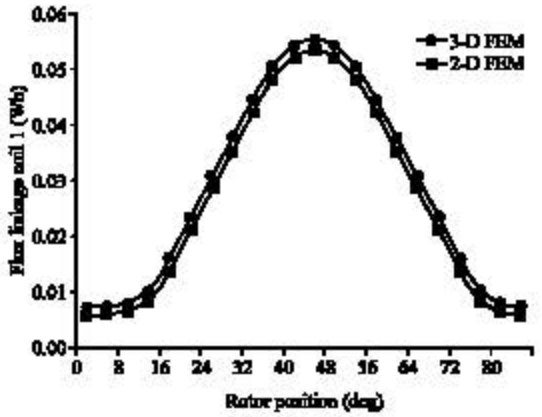

Fig. 6: Flux-linkage in coil one of phase A for 3-D and 2-D FEM

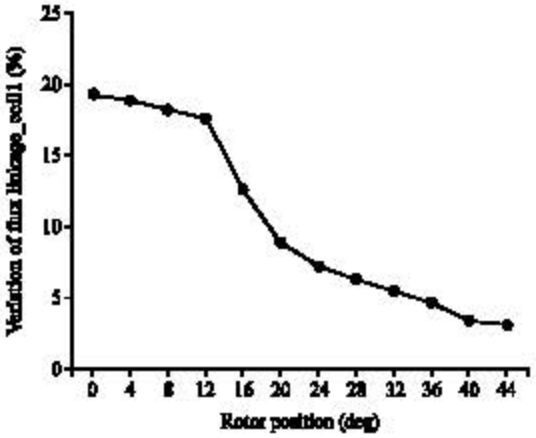

Fig. 7: Percentage of variation of flux-linkage in coil one of phase A for 3-D vs. 2-D FEM

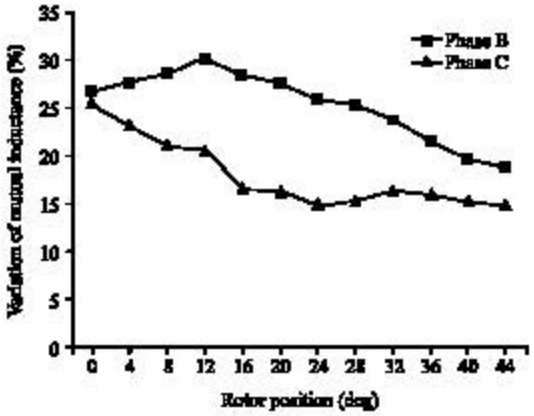

Fig. 8: Percentage of variation of mutual inductance in phase B, C for 3-D vs. 2-D FEM

The mutual inductance is defined as the ratio of flux-linking that phase to the exciting current in the other phase. According to this definition the mutual inductance values for phases B and C for SR motor using 3-D/ 2-D FEM have been calculated and compared.

The variations of mutual inductances for phases B and C are presented in Fig. 8 for the motor carrying the rated current of 2.5 A.

Considering the end effects and axial fringing fields, Fig. 8 shows the value of mutual inductance of phase B and phase C increases from 19 to 30% and 15 to 25% utilizing 3-D FE compared with 2-D FE, respectively. These variations are due to the changes in mutual flux linkages of each coil in that phase.

The static torque developed by the motor is calculated from the ratio of change in the co-energy

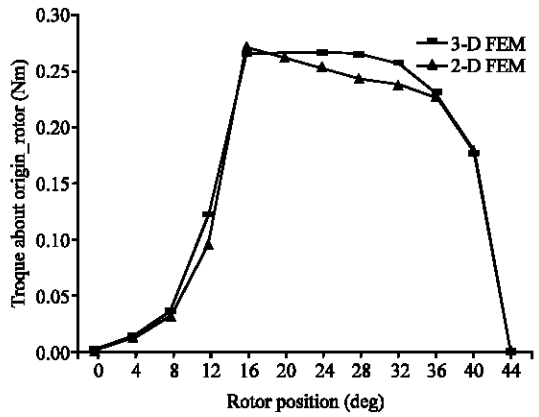

Fig. 9: Static torque of the motor vs. rotor position utilizing 3-D and 2-D FEM

Table 2: Percentage of Variation of static torque of the motor for 3-D vs. 2-D FEM

Degree	Variation (%)
0	15.61
4	14.93
8	15.03
12	27.74
16	-2.44
20	0.75
24	5.20
28	8.42
32	7.73
36	2.09
40	-1.14
44	0.23

respecting to the rotor position. The static torque versus rotor position for both 3-D and FEM is shown in Fig. 9.

Due to higher flux linkages in motor with 3-D FEM, the static torque obtained is also higher. Due to complete modeling of motor coil windings and consideration of the end effects plus axial fringing, the motor simulation in 3-D FEM is more precise and reliable than 2-D FEM simulation. Table 2 shows the comparison between 3-D and 2-D results for static torque.

According to Table 2, when the rotor rotates from aligned to unaligned position, the variation of static torque for 3-D FE analysis has 27.7% higher values than the 2-D FE analysis in peak.

Results of fundamental harmonic analysis of the static torque profiles for 3-D/2-D FEM in various eccentricities are obtained using MATLAB software. These results show that with using comprehensive method FE, the fundamental harmonic has 4.6% higher value than 2-D method. But it is observed that the 3rd, 5th and 7th harmonic torques for 3-D FE analysis has 7.7%, 9.8 and 21.5% lower values than the 2-D FE analysis, respectively.

CONCLUSION

Using finite element method is a valuable tool for magnetic design and performance calculations of switched reluctance motor parameters.

This study can be accounted for as a comprehensive study of performance characteristics analysis by 3-Dimensional as well as 2-D finite element method in switched reluctance motor. In this study, flux density, flux-linkage, terminal inductance, mutual inductance and torque profile in switched reluctance motor with 3-D FEM were analyzed and these characteristics analyzed with 2-D FEM. Then the results were compared with those obtained from 2-D FEM.

The different values of flux densities were obtained in excited stator poles and the corresponding rotor poles. This analysis shows that with the utilization of 3-D FEM, the values of the flux-linkage and mutual inductance per phase are increased in comparison with 2-D FEM. The computed results show that the torque profile of the motor under 3-D FE analysis has 27.7% higher values than the 2-D FE analysis in peak and the 3rd, 5th and 7th harmonic torques for 3-D FE analysis has lower values than the 2-D FE analysis.

The variations between 3-D/2-D FE results are due to the consideration of the end effects and also axial fringing field in 3-D FE analysis. Both method have been tested on 6/4 switched reluctance motor. From the obtained results, it has been shown that the 3-D approach is found to be a precise and successful method.

REFERENCES

Dorrell, D.G., I. Chindurza and C. Cossar, 2005. Effects of rotor eccentricity on torque in switched reluctance machines. IEEE Trans. Magnetics, 41: 3961-3963.

Geldhof, K.R., T.J. Vyncke, F.M.L.L. De Belie, L. Vandevelde, J.A.A. Melkebeek and R.K. Boel, 2007. Embedded Runge-Kutta methods for the integration of a current control loop in an SRM dynamic finite element model. IET Sci. Measurement Technol., 1: 17-20.

Hannoun, H., M. Hilairet and C. Marchand, 2007. Analytical modeling of switched reluctance machines including saturation. IEEE Int. Conf. Electric Mach. Drives, 1: 564-568.

Husain, I., A. Radun and J. Nairus, 2000. Unbalanced force calculation in switched-reluctance machines. IEEE Trans. Magnetics, 36: 330-338.

Kamper, M.J., S.W. Rasmeni and R.J. Wang, 2007. Finite-element time-step simulation of the switched reluctance machine drive under single pulse mode operation. IEEE Trans. Magnetics, 43: 3202-3208.

Magnet CAD Package, 2007. User Manual. Infolytica Corporation Ltd., Montreal, Canada.

Miller, T.J., 1993. Switched Reluctance Motors and their Controls. 1st Edn. Magna Physics Publishing and Clarendon Press, Oxford, London, pp: 13-89.

Ozoglu, Y., M. Garip and E. Mese, 2005. New pole tip shapes mitigating torque ripple in short pitched and fully pitched switched reluctance motors. Electric Power Syst. Res., 74: 95-103.

Parreira, B., S. Rafael, A.J. Pires and P.J.C. Branco, 2005. Obtaining the magnetic characteristics of an 8/6 switched reluctance machine: From FEM analysis to the experimental tests. IEEE Trans. Ind. Elect., 52: 1635-1643.

Sadiku, M.N.O., 2000. Numerical Techniques in Electromagnetics. CRC Press, New York, US.

Sheth, N.K., A.R.C. Sekharbabu and K.R. Rajagopal, 2006. Effects of inter-turn fault in phase winding on the performance of multi-phase doubly salient motors. J. Magnetism Magnetic Mater., 304: 207-209.

Sixdenier, F., L. Morel and J.P. Masson, 2006. Introducing dynamic behaviour of magnetic materials into a model of a switched reluctance motor drive. IEEE Trans. Magnetics, 42: 398-404.